Stanley K. Yoo, BS
Richard Watts, PhD
Priscilla A. Winchester, MD
Ramin Zabih, PhD
Yi Wang, PhD
Martin R. Prince, MD, PhD

Index terms:
Magnetic resonance (MR), image processing, 9∗.12942[2], ∗∗.12942[3]
Magnetic resonance (MR), vascular studies, 9∗.12942, ∗∗.12942

Published online before print
10.1148/radiol.2222010608
Radiology 2002; 222:564–568

Abbreviations:
CNR = contrast-to-noise ratio
DSA = digital subtraction angiography
2D = two-dimensional

[1] From the Department of Radiology MR Research, Weill Medical College of Cornell University, 515 E 71st St, Suite S120, New York, NY 10021. Received March 14, 2001; revision requested April 27; revision received June 27; accepted July 24. Supported in part by the American Heart Association-Heritage (grant 9951018T) and the National Institutes of Health (grants R01 HL60879, R01 HL62994). **Address correspondence to** Y.W. (e-mail: *yiwang@med.cornell.edu*).
[2] 9∗. Vascular system, location unspecified
[3] ∗∗. Multiple body systems

Author contributions:
Guarantors of integrity of entire study, Y.W., M.R.P.; study concepts, Y.W., M.R.P.; study design, R.Z., Y.W., M.R.P., R.W.; literature research, Y.W., S.K.Y.; clinical studies, P.A.W., M.R.P., R.W., Y.W.; data acquisition, R.W., P.A.W., M.R.P.; data analysis/interpretation, R.W., S.K.Y., P.A.W., M.R.P., Y.W.; statistical analysis, R.Z., S.K.Y., Y.W.; manuscript preparation, S.K.Y., Y.W., M.R.P.; manuscript definition of intellectual content, R.Z., Y.W., M.R.P.; manuscript editing, S.K.Y., Y.W., M.R.P.; manuscript revision/review and final version approval, Y.W., M.R.P.

Postprocessing Techniques for Time-resolved Contrast-enhanced MR Angiography[1]

The purpose of this study was to improve dynamic two-dimensional projection magnetic resonance digital subtraction angiography by using remasking and filtering postprocessing techniques. Four methods were evaluated in 50 patients: default mask subtraction, remasked subtraction, filtering based on the SD, and linear filtering. The results demonstrated that postprocessing techniques such as linear filtering can reduce background motion artifacts and improve arterial contrast-to-noise ratio.

Magnetic resonance (MR) angiography is increasingly used to help diagnose peripheral vascular disease, particularly in patients with contraindications to iodinated contrast material or arterial catheterization (1–6). Contrast material–enhanced MR angiography with the three-dimensional bolus-chase technique (6–13) has been particularly useful because it reduces the imaging time to a few minutes to cover the entire peripheral vasculature. It also reduces the dose of contrast material required because multiple stations are acquired during a single injection of MR contrast material, which is analogous to bolus-chase conventional digital subtraction angiography (DSA). However, despite recent developments in gradient speed and k-space sampling, accuracy is limited below the knees where the arteries are smaller in caliber and the bolus synchronization is less reliable as timing is optimized for the pelvis (13).

For this reason, we have found it useful to supplement the bolus-chase examination with preliminary two-dimensional (2D) MR DSA of the trifurcation and feet (13–16). It requires only 5–7 mL of gadolinium-based contrast material for the trifurcation and thus does not significantly interfere with performing a three-dimensional bolus-chase examination subsequently. Bolus timing information from 2D MR DSA is also helpful in planning the subsequent three-dimensional bolus-chase examination. Projection MR angiography of the trifurcation provides only a single anteroposterior view, but it can be performed repeatedly at 1–2-second intervals to help evaluate the time course and symmetry of vascular enhancement. It involves acquiring at least one projection image prior to the arrival of the contrast material to use as a mask for subtraction of the background signal. In these ways, it is similar to conventional DSA.

In conventional DSA, postprocessing techniques including remasking, filtering, and pixel shifting are commonly used to improve image quality. It would be valuable to assess the benefits of these techniques for MR DSA. Because MR data are complex (vector), unlike radiographic data, which are real numbers, these postprocessing techniques have to be generalized to the complex domain. The purpose of this study was to evaluate remasking and filtering postprocessing techniques for time-resolved MR DSA.

Materials and Methods

Patients

Fourier data from 2D MR DSA of the trifurcation in 50 consecutive patients undergoing peripheral MR angiography from September 11 to November 25, 2000, were evaluated with and without averaging. This study was approved by our institutional review board; informed consent was not required. These patients included 29 men (age range, 24–87 years; mean age, 70 years) and 21 women (age range, 33–85 years; mean age, 68 years). The primary indications for pe-

TABLE 1
Summary of CNR Measurements

Image	CNR	
	Mean	SD
Default	30.3	12.4
Remasked	30.0	12.5
SD	83.4	41.6
Linear	68.5	24.7

Note.—Default = peak arterial phase image from the default mask subtraction, linear = linearly filtered image, remasked = peak arterial phase image from the remasked subtraction, SD = SD image.

TABLE 2
Summary of CNR Differences with Corresponding Statistical Significance

Image	CNR Difference in Mean	*P* Value
Remasked-default	−0.3	.9
SD-default	53.1	<.001
SD-remasked	53.4	<.001
Linear-default	38.2	<.001
Linear-remasked	38.5	<.001
SD-linear	14.9	<.001

Note.—Default = peak arterial phase image from the default mask subtraction, linear = linearly filtered image, remasked = peak arterial phase image from the remasked subtraction, SD = SD image.

TABLE 3
Summary of Image Quality Comparison Results on the Five-Point Scale and Corresponding Statistical Significance

Image Quality Distribution	Scale					*P* Value for Image Quality
	−2	−1	0	1	2	
Reader 1						
Remasked versus default	0	4	33	11	2	~.3
SD versus default	0	2	5	31	12	<.003
SD versus remasked	0	2	12	32	3	<.003
Linear versus default	0	0	1	25	24	<.003
Linear versus remasked	0	0	0	27	23	<.003
Linear versus SD	0	9	19	20	2	~.06
Reader 2						
Remasked versus default	0	5	31	10	4	~.15
SD versus default	3	0	1	27	19	<.003
SD versus remasked	0	1	1	29	19	<.003
Linear versus default	0	0	1	28	21	<.003
Linear versus remasked	0	0	1	32	17	<.003
Linear versus SD	2	5	12	28	3	<.003

Note.—Default = peak arterial phase image from the default mask subtraction, linear = linearly filtered image, remasked = peak arterial phase image from the remasked subtraction, SD = SD image. −2 = one image was substantially worse than the other, −1 = one image was modestly worse than the other, 0 = one image was approximately the same as the other, 1 = one image was modestly better than the other, 2 = one image was substantially better than the other.

ripheral MR angiography in these patients included claudication (n = 26), limb-threatening ischemia (n = 13), aneurysm (n = 7), bypass graft placement (n = 3), and dissection (n = 1).

Imaging

All data were obtained at 1.5 T by using the head coil for signal transmission and reception (LX Horizon; GE Medical Systems, Milwaukee, Wis). The patients were placed feet first into the magnet, with their legs positioned within the head coil to image from above the patella down to the middle of the calf. A sagittal gradient-echo scout sequence was used to position the coronal 2D projection MR angiographic slab so that it encompassed the entire calf. Two-dimensional projection MR angiography was performed as a coronal spoiled gradient-echo sequence by using the following parameters: 10/2 (repetition time msec/echo time msec); flip angle, 60°; slab thickness, 7–10 cm; field of view, 30 cm; matrix, 256 × 192; bandwidth, 16 kHz. The imaging time was 1.95 seconds per acquisition for a total of 68 seconds to repeat the acquisition 35 times.

Five to seven milliliters of 0.5 mol/L gadolinium-based contrast material (gadopentetate dimeglumine, Magnevist, Berlex Laboratories, Wayne, NJ or gadodiamide, Omniscan, Nycomed Amersham, Princeton, NJ) was injected and flushed with 20 mL of saline. The injection rate was 2.5 mL/sec and was performed with an automatic injector or by hand. The injection was initiated simultaneously with initiating the imaging. In this way, at least five to 10 mask images were obtained before administration of the contrast material and prior to the arrival in the arterial phase at the trifurcation.

Postprocessing Techniques

Our approach to generalize postprocessing techniques to the complex domain was to treat the two orthogonal components of MR data separately and equivalently, apply postprocessing techniques of real numbers to each component, and combine the two processed components. In this study, we focused on remasking and filtering methods.

Remasking.—The purpose was to identify a mask that was closest to the background of the enhanced peak arterial phase image so that motion artifacts were minimized on the subtracted arterial phase images. This was achieved through two iterations of subtraction. First, subtraction by using a default mask (image 5 of the 35 serial images) was performed to identify the peak arterial phase (maximal arterial signal). Then the identified peak arterial phase image was used as a mask, and subtraction was performed again to identify the optimal mask among the images obtained before contrast enhancement (ie, the one with minimal background).

Filtering.—A widely used filtering technique is matched filtering, which sums a time series of images into a single image of optimal contrast-to-noise ratio (CNR) with undesired background signal suppressed (17–19). The linearly matched filter requires an input of signal waveform that characterizes the arterial signal. However, such an arterial waveform is not well defined throughout the field of view because of variations in the time the contrast material reaches the arteries, particularly portions of an artery distal to

stenosis, small branch arteries, and arteries filled with retrograde flow.

This problem was overcome with the generalized local matched filter, which replaced the global arterial waveform with a local arterial curve defined by the pixel value minus its mean. This provides simple automated filtering. Let the final image be s, the time series S_n, and its average $\bar{S}$, and then the local matched filtered image is calculated as follows, which is equivalent to taking the SD (19):

$$\{\mathrm{Re}[s(x, y)]\}^2 = \sum_n \{\mathrm{Re}[S_n(x, y)] - \mathrm{Re}[\bar{S}(x, y)]\}^2/N$$

$$\{\mathrm{Im}[s(x, y)]\}^2 = \sum_n \{\mathrm{Im}[S_n(x, y)] - \mathrm{Im}[\bar{S}(x, y)]\}^2/N$$

$$|s(x, y)| = \langle\{\mathrm{Re}[s(x, y)]\}^2 + \{\mathrm{Im}[s(x, y)]\}^2\rangle^{1/2},$$

where Re = real part, x and y = in-plane coordinates, n = image index, Im = imaginary part, and N = the total number of images in the series. This filtered image is referred to as the SD image. In this study, the summation range was limited to exclude images with venous or background enhancement.

On this semiautomated SD image, all images were used from the first mask to the last arterial phase, and it was prone to artifacts caused by motion that occurred during imaging. Such motion artifacts are common at peripheral MR angiography, as the legs tremble in most older patients. As a first attempt to eliminate motion artifacts, simple linear filtering of a manually selected mask image set *(M)* and arterial phase image set *(A)* was used to generate a linearly filtered image:

$$s_h(x, y) = \sum_{n\in A} S_n(x, y)/N_A - \sum_{n\in M} S_n(x, y)/N_M.$$

Image Evaluation

The peak arterial phase image from the default mask subtraction (default) and from the remasked subtraction (remasked), the SD image (SD), and the linearly filtered image (linear) were evaluated by using an objective CNR and a subjective image quality score.

CNR was measured in the following manner. The vessel signal intensity was the average of the maximal signal intensity of a transverse line over all transverse lines on an image. Noise was the SD of the signal intensity in a background region. The CNR was the difference between vessel signal intensity and the mean of background signal intensity divided by the SD of the latter. In addition, the first and second order branches of the geniculate, anterior tibial, posterior tibial, and peroneal arteries were also identified independently by two experienced vascular radiologists (M.R.P., P.A.W.).

Paired comparisons of the four postprocessed images—default, remasked, SD, and linear—for a total of six pairs, were performed by the same two MR radiologists to assess the differences in image quality by using a five-point scale: 2, one image was substantially better than the other; 1, one image was modestly better than the other; 0, one image was approximately the same as the other; −1, one image was modestly worse than the other; −2, one image was substantially worse than the other. The image pairs were presented randomly, and the two radiologists read the images independently.

Statistical Analysis

The significance of differences in a paired comparison was assessed by performing the paired two-sample t test by using the two sets of CNR measurements and by performing the paired Wilcoxon signed rank test over the image quality difference score set (20). The Bonferroni correction was applied to the P value to account for the nature of multiple comparisons (21).

TABLE 4
Summary of Arteries Visualized by the Readers

Arteries	Images			
	Default	Remasked	SD	Linear
Visualized by Reader 1				
Geniculate	25	26	37	41
Branch 1	5	6	15	19
Branch 2	0	0	4	3
Anterior tibial	40	42	46	44
Branch 1	10	10	23	23
Branch 2	0	0	3	0
Posterior tibial	35	36	43	42
Branch 1	8	9	28	23
Branch 2	0	0	4	5
Peroneal	41	41	42	45
Branch 1	7	8	17	21
Branch 2	0	0	1	0
Visualized by Reader 2				
Geniculate	30	32	39	42
Branch 1	4	6	12	13
Branch 2	0	0	1	3
Anterior tibial	42	43	43	44
Branch 1	8	10	18	15
Branch 2	0	0	1	0
Posterior tibial	38	39	39	39
Branch 1	14	11	19	21
Branch 2	0	0	1	5
Peroneal	43	43	43	45
Branch 1	6	6	18	17
Branch 2	0	0	0	1

Note.—Default = peak arterial phase image from the default mask subtraction, linear = linearly filtered image, remasked = peak arterial phase image from the remasked subtraction, SD = SD image.

TABLE 5
Summary of Image Artifact Occurrence

Image	No. of Artifacts Observed	
	Reader 1	Reader 2
Default	23	22
Remasked	15	16
SD	14	14
Linear	14	15

Note.—Default = peak arterial phase image from the default mask subtraction, linear = linearly filtered image, remasked = peak arterial phase image from the remasked subtraction, SD = SD image.

Results

The CNR data are tabulated in Table 1, and the comparisons are tabulated in Table 2. The average CNRs for the peak ar-

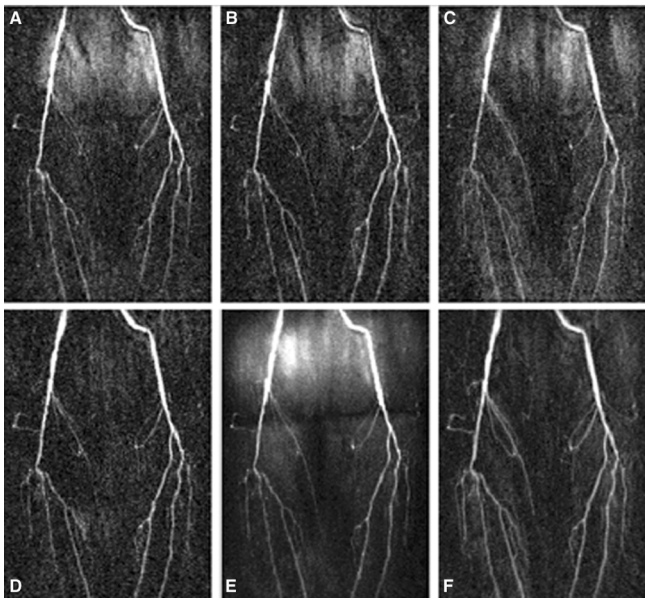

Figure 1. Coronal 2D MR DSA (10/2; flip angle, 60°) images obtained in a 75-year-old man with claudication. *A–C,* Contiguous arterial phase images in which the default mask was used. *D,* Peak arterial phase image (corresponding to *B)* in which an optimized mask was used. *E,* Filtered image with SD from the first mask to the last arterial phase images. *F,* Linearly filtered image in which manually selected masks (five nonenhanced images) and arterial phases (three arterial phases depicted in *A–C)* were used. The remasked image *(D)* demonstrates substantial reduction in background motion artifacts, as compared with that on the default image *(B).* Both the SD image *(E)* and the linearly filtered image *(F)* demonstrate improved CNR and better vascular details, but the background artifacts are suppressed on the linear image *(F).*

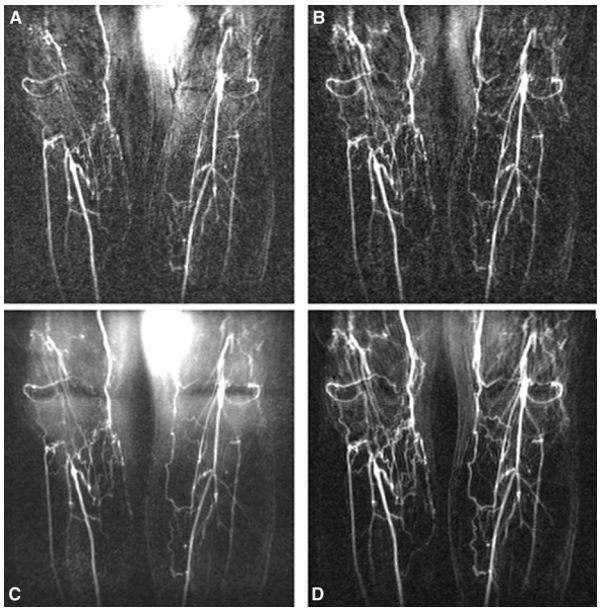

Figure 2. Coronal 2D MR DSA (10/2; flip angle, 60°) images obtained in a 67-year-old man with right calf claudication. *A,* Arterial phase image in which the default mask was used. *B,* Peak arterial phase image (corresponding to *A)* in which an optimized mask was used. *C,* Filtered image with SD from the first mask to the last arterial phase images. *D,* Linearly filtered image in which manually selected masks (10 nonenhanced images) and arterial phases (four arterial phases) were used. The motion artifact is substantially suppressed on the remasked image *(B)* and the linearly filtered image *(D).*

terial phase images from default subtraction (default) and remasked subtraction (remasked) were approximately the same ($P = .9$). Both the SD image (SD) and the linearly filtered image (linear) had significantly higher (greater than twofold) CNR than did the default and remasked images ($P < .001$), as many images were summarized. The linearly filtered image also had significantly lower CNR than did the SD image ($P < .001$), as fewer images were used in the linear filtering.

In the image quality comparison (Table 3), both readers 1 and 2 regarded the linearly filtered and SD images to be significantly better than both the default and remasked images ($P < .003$). The linearly filtered images were judged to be better than the SD images ($P \sim .06$ for reader 1 and $P < .003$ for reader 2). Remasked images yielded slightly but not significantly better image quality than did the default mask images according to both readers ($P \sim .3$ for reader 1 and $P \sim .15$ for reader 2).

Vessel visibility was higher on the SD and linearly filtered images than on either the default or remasked images (Table 4). For linearly and SD filtered images, the first order branch vessels of the geniculate, anterior tibial, posterior tibial, and peroneal arteries were seen at least twice as often as they were seen on either the default or remasked images. There were instances in which the second order branches of these arteries were observed on the linear or SD images but never on the default or remasked images. Differences were less discernable in vessel visibility between SD and linear images. SD and linearly filtered images displayed less motion artifact than did both remasked and default mask images (Table 5), while remasked images displayed less motion artifact than did the default mask images.

Figure 1 demonstrates an instance in which the remasked image (Fig 1, *D)* eliminated much of the background motion artifact on the arterial phase images created by using the default mask (Fig 1, *A–C).* Vessel depiction improved on the linearly filtered image (Fig 1, *F),* as compared with that on any of the individual arterial phase images. Linear filtering showed second order branches off the geniculate and posterior tibial arteries, whereas second order branches off these arteries were not seen on either default or remasked images (Fig 1, *A–D).* The SD image (Fig 1, *E)* also demonstrated improved vessel definition and showed second order branches off the geniculate and posterior tibial arteries, though motion artifact remained.

Figure 2 demonstrates the advantage of manually selecting an optimized mask over using an arbitrary default mask. The motion artifact seen in the upper portion of the arterial phase images of default mask (Fig 2, *A)* was substantially reduced by remasking (Fig 2, *B),* which also made the geniculate branches more visible. The almost automated SD image (Fig 2, *C)* contained motion artifacts, which were substantially reduced on the linearly filtered image (Fig 2, *D).*

Figure 3 is an example in which images in a patient with slow arterial blood flow benefit from the single linearly filtered image. Individual default arterial phase images for this patient yielded poor CNR and vessel visibility (Fig 3, *A).* However, the SD and linearly filtered images (Fig 3, *C, D)* showed increased visibility of the geniculate artery and branches off the posterior tibial artery in comparison with that on the default and remasked images (Fig 3, *A,*

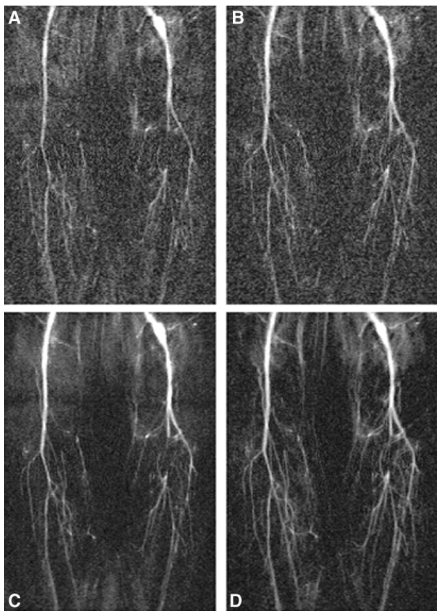

Figure 3. Coronal 2D MR DSA (10/2; flip angle, 60°) images obtained in a 24-year-old man with a nonhealing ulcer. *A,* Arterial phase image in which the default mask was used. *B,* Peak arterial phase image (corresponding to *A)* in which an optimized mask was used. *C,* Filtered image with SD from the first mask to the last arterial phase images. *D,* Linearly filtered image in which manually selected masks (nine nonenhanced images) and arterial phases (four arterial phases) were used. Both filtered images *C* and *D)* demonstrate substantial improvement in vascular CNR.

B). The CNRs of the linearly filtered and SD images were more than twofold greater than those of the default mask or remasked images.

Discussion

These data in 50 consecutive patients undergoing peripheral MR angiography demonstrate that postprocessing can improve 2D MR DSA image quality, in concordance with the experience of radiographic DSA. Remasking can reduce motion artifacts on peak arterial phase images. Filtered images can summarily depict vascular anatomy in the time series images conveniently on a single image with significantly higher CNR.

The ability to have a single summary image reflecting the best depiction of vascular anatomy may reduce the time required to analyze a case by having to look at only a single image. Of course, the arterial phase images could be displayed as a video loop and provide equivalent or more information to the observer than would a summary image. Presumably, a human can perform averaging equivalent to linear or SD filtering by integrating the information of multiple images projected rapidly in sequence, and this might be superior to using the computer to generate a single composite image. This would be especially true in the event of motion that results in vessel blur when misregistered images are averaged. However, the summary image does not diminish but adds to the value of the time series images. Even the video loop display method would benefit from filtering by using a mask of reduced noise obtained by averaging multiple masks. Furthermore, there are many instances in which video is not available—for example, on the view box in an operating room.

The semiautomated local matched filtered image (SD image) demonstrates arterial anatomy superior to that on the individual peak arterial phase image but inferior to that on the linearly filtered image. This may be attributed to motion artifacts. Individual mask and arterial phase images with motion effects, which were included on the SD image but excluded on the linearly filtered image, though improving CNR, introduce motion noise that diminishes the conspicuity of small arteries on the SD image.

Motion artifacts are prevalent problems; however, the simple pixel-shifting method used in x-ray DSA cannot be generalized directly to MR DSA, in which data are acquired in complex k space. Motion effects can be corrected for by detecting motion displacement and compensating for the phase shifts for each individual echo, a task of complexity beyond the scope of this article (22). The simple linearly filtered image provides reduction in motion artifacts and improvement in vascular delineation, and it may serve as a simple and practical tool for summarizing images. The linear filtering can be regarded as motion gating in that images with substantial motion are discarded from summation. Currently, we are working on motion detection algorithms to fully automate motion gating. In summary, postprocessing methods such as remasking and filtering can be used to reduce motion effects and summarize vascular anatomy on a single high CNR image obtained by means of dynamic 2D MR DSA.

References

1. Owen RS, Carpenter JP, Baum RA, Perloff LJ, Cope C. Magnetic resonance imaging of angiographically occult runoff vessels in peripheral arterial occlusive disease. N Engl J Med 1992; 326:1577–1581.
2. Yucel EK, Kaufman JA, Geller SC, Waltman AC. Atherosclerotic occlusive disease of the lower extremity: prospective evaluation with two-dimensional time-of-flight MR angiography. Radiology 1993; 187:637–641.
3. Korosec FR, Frayne R, Grist TM, Mistretta CA. Time-resolved contrast-enhanced 3D MR angiography. Magn Reson Med 1996; 36:345–351.
4. Prince MR, Grist TM, Debatin JF. 3D contrast MR angiography. 2nd ed. New York, NY: Springer-Verlag, 1998.
5. Rofsky NM, Adelman MA. MR angiography in the evaluation of atherosclerotic peripheral vascular disease. Radiology 2000; 214: 325–338.
6. Ho KY, Leiner T, de Haan MW, Kessels AG, Kitslaar PJ, van Engelshoven JM. Peripheral vascular tree stenoses: evaluation with moving-bed infusion-tracking MR angiography. Radiology 1998; 206:683–692.
7. Wang Y, Lee HM, Khilnani NM, et al. Bolus-chase MR digital subtraction angiography in the lower extremity. Radiology 1998; 207: 263–269.
8. Wang Y, Lee HM, Avakian R, Winchester PA, Khilnani NM, Trost D. Timing algorithm for bolus chase MR digital subtraction angiography. Magn Reson Med 1998; 39:691–696.
9. Ho VB, Choyke PL, Foo TK, et al. Automated bolus chase peripheral MR angiography: initial practical experiences and future directions of this work-in-progress. J Magn Reson Imaging 1999; 10:376–388.
10. Meaney JF, Ridgway JP, Chakraverty S, et al. Stepping-table gadolinium-enhanced digital subtraction MR angiography of the aorta and lower extremity arteries: preliminary experience. Radiology 1999; 211:59–67.
11. Ruehm SG, Hany TF, Pfammatter T, Schneider E, Ladd M, Debatin JF. Pelvic and lower extremity arterial imaging: diagnostic performance of three-dimensional contrast-enhanced MR angiography. AJR Am J Roentgenol 2000; 174:1127–1136.
12. Earls JP, DeSena S, Bluemke DA. Gadolinium-enhanced three-dimensional MR angiography of the entire aorta and iliac arteries with dynamic manual table translation. Radiology 1998; 209:844–849.
13. Wang Y, Winchester PA, Khilnani NM, et al. Contrast enhanced peripheral MRA from abdominal aorta to pedal arteries: combined dynamic 2D and bolus chase 3D acquisitions. Invest Radiol 2001; 36:170–177.
14. Wang Y, Johnston DL, Breen JF, et al. Dynamic MR digital subtraction angiography using contrast enhancement, fast data acquisition, and complex subtraction. Magn Reson Med 1996; 36:551–556.
15. Hennig J, Schefler K, Laubenberger J, Strecker R. Time-resolved projection angiography after bolus injection of contrast agent. Magn Reson Med 1997; 37:341–345.
16. Winchester PA, Lee HM, Khilnani NM, et al. Comparison of two-dimensional MR digital subtraction angiography of the lower extremity with x-ray angiography. J Vasc Interv Radiol 1998; 9:891–900.
17. Kruger RA, Riederer SJ. Digital subtraction angiography. Boston, Mass: Hall Medical, 1984; 197–219.
18. Kruger RA. A method for time domain filtering using computerized fluoroscopy. Med Phys 1981; 8:466–470.
19. Wang Y, Weber DM, Korosec FR, et al. Generalized matched filtering for time-resolved MR angiography of pulsatile flow. Magn Reson Med 1993; 30:600–608.
20. Zar JH. Biostatistical analysis. 3rd ed. Upper Saddle River, NJ: Prentice Hall, 1996; 123–178.
21. SISA. Bonferroni adjustment online. Available at: *http://home.clara.net/sisa/bonfer.htm.* Accessed November 2001.
22. Ehman RL, Felmlee JP. Adaptive technique for high-definition MR imaging of moving structures. Radiology 1989; 173:255–263.